INFLUENCE OF YAW MISALIGNMENT DIRECTION AND CORIOLIS FORCE ON THE WAKE CHARACTERISTICS OF A WIND TURBINE

Utkarsh Deep Tiwari
Department of Chemical Engineering
Indian Institute of Technology Hyderabad
Kandi, Sangareddy, Telangana 502284, India
ch21resch11008@iith.ac.in

Niranjan S Ghaisas
Department of Mechanical and Aerospace Engineering
Indian Institute of Technology Hyderabad
Kandi, Sangareddy, Telangana 502284, India
nghaisas@mae.iith.ac.in

Kishalay Mitra
Department of Chemical Engineering
Indian Institute of Technology Hyderabad
Kandi, Sangareddy, Telangana 502284, India
kishalay@che.iith.ac.in

ABSTRACT

We study the effect of yaw misalignment direction and Coriolis force-induced wind veer direction on the wake structure of a utility-scale wind turbine operating under the effect of Coriolis forces through large-eddy simulations (LES). We analyze scenarios with yaw angles $\gamma = +30^\circ$, 0° and -30° (rotor-plane rotated counter-clockwise, not rotated and rotated clockwise, respectively, when viewed from above). For each scenario, we consider the turbine to be located in the Northern hemisphere at latitude $\beta = 41.3^\circ$, on the equator ($\beta = 0^\circ$) and in the Southern hemisphere at $\beta = -41.3^\circ$. The results demonstrate that the Coriolis force introduces a notable asymmetry in the wake structure depending on the latitude and on the yaw direction. In the northern hemisphere, for $\gamma = -30^\circ$, the wake exhibits a distinct curled or kidney-shaped cross-section, whereas the $\gamma = +30^\circ$ case produces a wake shape that is closer to a Gaussian. Similar complementary shapes are seen for a yawed turbine located in the southern hemisphere at the same latitude magnitude. An analytical model that incorporates turbine yaw and Coriolis-induced wind veer effects is evaluated. While the broad features of the wake shape are found to be quite similar, the wake extents are smaller in the model predictions than in the LES. The velocity deficit along the centerline is predicted reasonably correctly for all cases, while the sensitivity of the power predictions to the latitude is not captured by the model, highlighting the need for model enhancements to account for these effects in future studies.

INTRODUCTION

Efficient utilization of wind energy installations demands a clear understanding of wind turbine wakes within the atmospheric boundary layer (ABL). Wake interactions reduce power and increase fatigue loads, motivating active control strategies such as yaw misalignment to deflect them and enhance farm performance (Fleming *et al.*, 2014). In the ABL, the Coriolis force leads to wind veer, i.e. a horizontal component of velocity that is also tangential to the turbine rotor plane, and creates a skewed wake structure for utility-scale turbines (Abkar & Porté-Agel, 2016; Heck & Howland, 2025). Yawing a turbine leads to the formation of a counter-rotating vortex pair (CVP) and the formation of a 'kidney-shaped' wake behind the turbine (Howland *et al.*, 2016; Mohammadi *et al.*, 2022). The superposition of veer-induced skewing and yaw-induced CVPs produces complex wake asymmetries that challenge analytical models (Mohammadi *et al.*, 2022). While yaw and Coriolis effects have been studied separately (Abkar & Porté-Agel (2016); Tiwari *et al.* (2025)), their combined influence, particularly for turbines yawed in opposite directions for the same direction of Coriolis forcing, has not been studied systematically.

This work addresses this gap using large-eddy simulation (LES) of the flow over a utility-scale wind turbine sited in a conventionally neutral ABL. The shape of the wake is shown to be qualitatively different for the same Coriolis forcing but with yawing the turbine in opposite directions. The effect of changing the latitude, which leads to different magnitudes of wind veer, and changes in the Coriolis forcing is explored. Implications of the resulting asymmetries on analytical modeling of the wake are discussed. Specifically, the analytical framework of Bastankhah *et al.* (2022) and Mohammadi *et al.* (2022) is evaluated for a range of positive, zero and negative latitudes along with a range of positive, zero and negative yaw misalignment angles.

METHODOLOGY

Simulations are performed using the OpenFOAM-based SOWFA solver (Churchfield *et al.*, 2012), which solves the incompressible-Boussinesq LES-filtered Navier-Stokes equations in a Cartesian box. Velocity components are denoted by (U,V,W) or equivalently u_i with $i = 1,2,3$ referring to the streamwise (x), spanwise (y) and vertical (z) directions, respectively. Buoyancy forces and Coriolis forces are included in the simulations, the latter through the term $-2\varepsilon_{ijk}\Omega_j u_k$, with the rotation vector $\overline{\Omega} = [0 \;\; \omega\cos\beta \;\; \omega\sin\beta]$. Here, $\omega \approx 7.29 \times 10^{-5}$ rad/s is the Earth's angular speed and β is the latitude where the simulation domain is placed. Subgrid-scale effects on the larger, resolved, scales are modeled through the one-equation LES model (Churchfield *et al.*, 2012). The simulations are conducted in two stages - a 'precursor' run and a 'turbine' run. The domain size in both runs is 6.3 km × 2.016 km × 1.008 km. The turbine model is the NREL 5 MW reference wind turbine with a diameter $D = 126$ m and hub-height $z_h = 90$ m, operated in Region II of its power curve with a fixed tip-speed ratio of 8.35. In terms of the turbine diameter, the cuboidal domain dimensions are $50D \times 16D \times 8D$ in x, y and z directions, respectively. The turbine is placed at a distance of $7D$ from the beginning of the domain along the x direction and at the mid-span location along the y direction and the origin of the Cartesian axes is collocated with this position.

In the precursor, horizontally periodic boundary conditions are maintained so as to allow the development of a fully-developed conventionally neutral turbulent boundary layer (CNBL). The CNBL flow in the precursor is driven by a geostrophic wind adjusted so as to maintain a speed of $U_{\infty,h} = 7.9$ m/s at the turbine hub-height. The angle of the geostrophic wind is also adjusted to maintain the hub-height velocity directed along the positive x axis. After a spinup of 1880 time units (1 time unit equals $D/U_{\infty,h}$, where $D = 126$ m is the turbine diameter), horizontally- and temporally-averaged statistics are collected over another 1880 time units. During this post-spinup phase, velocity and temperature fields at the $x = -7D$ plane (i.e. the start of the domain) are stored to disk. In the 'turbine' run, these velocity and temperature fields are applied as inflow conditions and the other horizontal boundaries are treated as outflow boundaries. The 'turbine' run is carried out for 1880 time units to allow development of a statistically stationary state, and time-averaging is performed over the subsequent 1725 time units to obtain well-converged statistics. Wind turbine forces exerted on the flow in the 'turbine' run are modeled using an actuator line model.

Three different 'precursor' simulations are conducted, at latitudes of $\beta = -41.3^\circ$, 0° and 41.3°. For each precursor run, three 'turbine' runs are conducted for turbine yaw misalignment angles $\gamma = -30^\circ$, 0° and $+30^\circ$. Here, γ is considered to be positive when the rotor is displaced in the anti-clockwise direction with respect to the incoming wind direction (positive x axis) when viewed from above.

The LES results are compared with the predictions of a vortex-sheet based analytical model of a yawed wind turbine wake subjected to veered inflow (Bastankhah *et al.* (2022); Mohammadi *et al.* (2022)). This modeling framework predicts the velocity deficit in the wake as

$$\frac{\Delta U(x,y,z)}{U_{\infty,h}} = \frac{\Delta U_c(x)}{U_{\infty,h}} \exp\left[-\frac{y^2 + (z - z_h)^2}{2\sigma(x,y,z)^2}\right], \qquad (1)$$

where ΔU_c is the centerline velocity deficit and σ is the wake width. The wake width is given by $\sigma = kx + 0.4\xi(x,\theta)$, where k is the wake expansion coefficient and ξ is the curled wake shape function with the polar angle $\theta = \tan^{-1}(z - z_h)/y$. The wake expansion coefficient is obtained from $k = \alpha_k u_*/U_{\infty,h}$, where α_k is an empirical constant and u_* is the inflow friction velocity. In each case below, α_k is obtained by requiring the centerline velocity deficit (shown later) to agree closely with the LES results. The modeling framework detailed in Bastankhah *et al.* (2022) provides expressions for ΔU_c and ξ incorporating effects of turbine yaw misalignment angle (γ). The modified framework described in Mohammadi *et al.* (2022) incorporates effect of wind veer, $\alpha(z) = \tan^{-1}(V(z)/U(z))$, that is induced by Coriolis forces that differ with differing latitudes, β. This modeling framework is evaluated using our LES results for a range of γ and β values below.

RESULTS AND DISCUSSION

This section presents a detailed analysis of how the turbine wake behaves under yaw misalignment in the presence of Coriolis effects. The discussion is organized by presenting the inflow conditions at the upstream of the turbine, the resulting wake structure, its recovery downstream, and its impact on wind farm performance. First, the contour line plots are used to describe the shape and spatial development of the wake. Next, the centerline velocity profiles are examined to understand how quickly the wake recovers and how this depends on yaw direction and latitude. Finally, these observations are linked to the expected power output of downstream turbines, highlighting the practical implications for wake steering strategies.

Inflow Profiles

Figure 1 shows the streamwise (U) and spanwise velocity (V) at the upstream of the turbine normalized by the horizontally averaged streamwise velocity at hub height ($U_{\infty,h}$), the wind veer angle ($\alpha = \tan^{-1}(V/U)$) and the turbulence intensity ($I = \sqrt{(2/3)TKE}/U$, where $TKE = (\overline{u_i' u_i'})/2$). The streamwise velocity and the turbulence velocity remain largely unaffected by changes in the latitude, β (Figure 1a, d). In contrast, latitude significantly influences the spanwise velocity (Figure 1b), thereby introducing wind veer. At the equator, $\beta = 0^\circ$, the spanwise velocity is negligible. For $\beta = 41.3^\circ$, the normalized spanwise velocity varies approximately from 0.02 to -0.02 from the bottom to the top of the rotor, with the direction reversing for $\beta = -41.3$. A corresponding trend is observed in the wind veer angle α (Figure 1c), with values varying over roughly 3° over the rotor extents. This wind veer is responsible for the distortion of the wind turbine wake downstream of the turbine.

Wake Shapes

Figure 2 shows contours of the velocity deficit at different x planes downstream of the turbine for the combination of non-yawed ($\gamma = 0^\circ$) turbine and three values of latitude. At the equator ($\beta = 0^\circ$), the wake shape remains almost exactly circular consistent with the fact that there is no spanwise inflow velocity for this case. The wake shape resembles an ellipse rather than a circle for non-zero latitudes due to the non-zero inflow wind veer in these cases. Specifically, for the latitude $\beta = 41.3^\circ$, the top of the wake skews to the left and the bottom skews to the right (Figures 2e, f, g, h). Skewing in the opposite sense is seen for $\beta = -41.3^\circ$ (Figures 2i, j, k, l) consistent with the direction of the spanwise velocity seen in Figure 1b. To identify the wake extent and shape, one specific contour level, $\Delta U/U_{\infty,h} = 0.1$, is highlighted from the LES data using inverted triangles. The same contour level obtained from model predictions is depicted in each plot using a black solid line. The analytical model largely succeeds at capturing the skewing of the wake in all cases seen in Figure 2. While the wake extents do not exactly agree at every azimuthal position, the overall extents of the chosen representative contour level are largely similar for the non-yawed turbine cases.

Figure 3 shows the wake of a turbine yawed by $\gamma = \pm 30^\circ$ placed on the equator ($\beta = 0^\circ$). Here, the wake shape resembles a kidney and this has been referred to previously as a 'curled' wake (e.g. Howland *et al.* (2016)). The wake shape

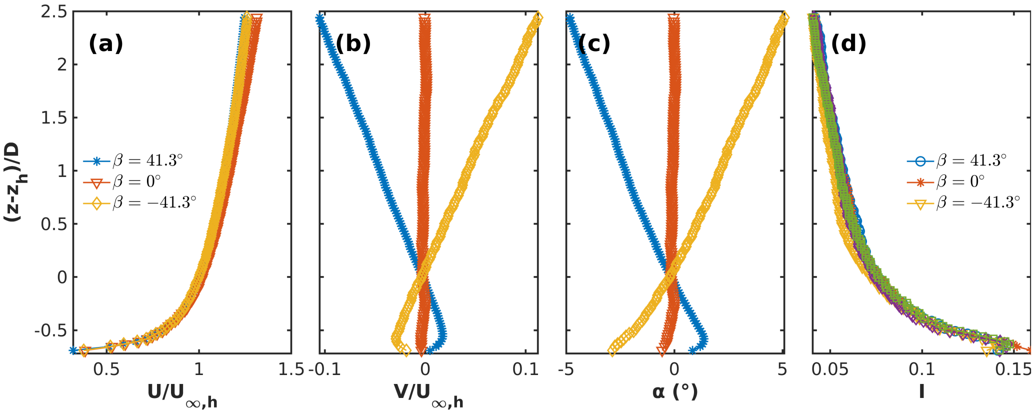

Figure 1. Variation of (a) non-dimensionalized streamwise velocity, (b) non-dimensionalized spanwise velocity, (c) wind veer and (d) turbulence intensity along the vertical direction upstream of the turbine.

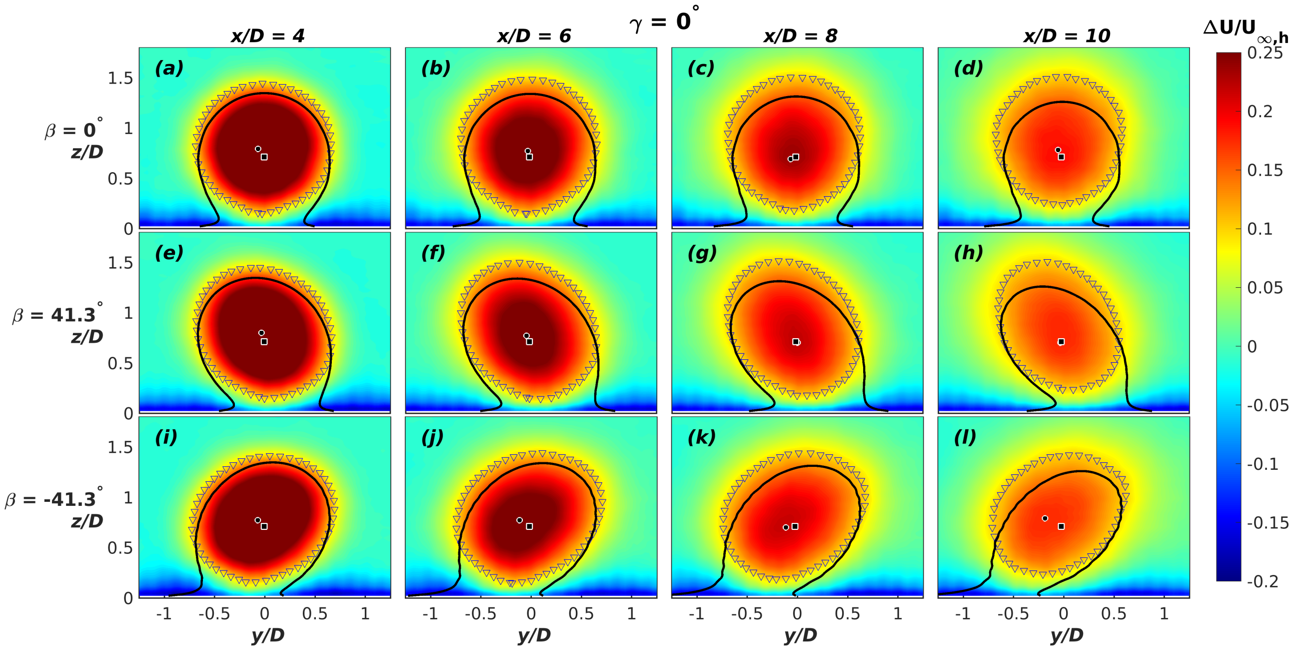

Figure 2. Spatial evolution of contours downstream of a non-yawed turbine ($\gamma = 0°$) located at the equator (a-d) $\beta = 0°$, (e-h) $\beta = 41.3°$, and (i-l) $\beta = -41.3°$, shown at (a, e, i) $x/D = 4$, (b, f, j) $x/D = 6$, (c, g, k) $x/D = 8$, and (d, h, l) $x/D = 10$. The blue triangle inverted triangles (∇) and the black solid line (–) show the contour line at $\Delta U/U_{\infty,h} = 0.1$ from the LES data and analytical model (with $\alpha_k = 0.5$), respectively.

is seen to be largely anti-symmetric about the vertical axis between the $\gamma = 30°$ and $-30°$ cases. This is expected from the governing equations where there is no influence of Coriolis forces and the turbine yaw direction is reversed between the $\gamma = 30°$ and $-30°$ cases. The analytical model framework predicts the general trend in the curled shape of the wake qualitatively correctly. However, the precise extents of the $\Delta U/U_{\infty,h} = 0.1$ contour levels do not agree between the LES and the model.

Figures 4 and 5 show wake contours when both effects, yaw misalignment and wind veer, are active simultaneously. Focusing on Figure 4 for $\beta = 41.3°$, clear qualitative differences are seen in the wake shape between the positively- and negatively-yawed turbine cases. For $\gamma = 30°$ (Figures 4a-d) the portion of the wake above the hub-height skews to the left, similar to the behavior observed for the $(\beta, \gamma) = (41.3°, 0°)$ case seen previously in Figure 2e-h. The lower portion of the wake shows an elongated and distorted 'tail' where the normalized deficit magnitude is small ($\Delta U/U_{\infty,h} < 0.1$). For $\gamma = -30°$ (Figures 4e-h), on the other hand, the curled wake shape is distinctly seen, similar to the shapes seen in Figure 3. A clear difference is also seen in the position of the wake centroid between the $\gamma = \pm 30°$ cases here. The differences between the wake shapes in the two cases are further quantified by determining the goodness of fit between the LES data and a simple two-dimensional Gaussian shape. The coefficient of determination (R^2) is calculated for the velocity deficits obtained from the LES and from Eq. (1) for a range of σ values and its maximum is noted. A perfect Gaussian shape would have $R^2_{max} = 1$ while a departure from unity indicates a departure from Gaussian shape. At $x/D = 8$ and 10, the $\gamma = 30°$ cases (Figures 4c, d) have a maximum goodness of fit, $R^2_{max} \approx 0.75$ while the $\gamma = -30°$ cases (Figures 4g, h) have a much smaller $R^2_{max} \approx 0.55$.

Figure 4 further shows that the wake shape predicted by the analytical model is broadly reasonable. However, the lateral and vertical deflection of the wake center location is significantly under-predicted in both cases. Similarly, the

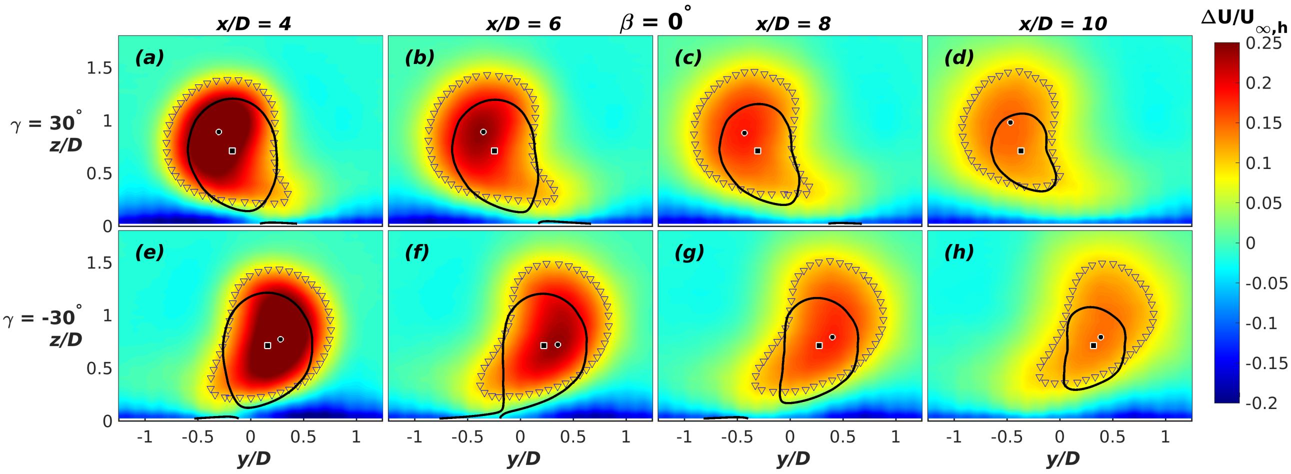

Figure 3. Spatial variation of contours downstream of a turbine yawed at, (a-d) $\gamma = 30°$ and (e-h) $\gamma = -30°$ located at latitude $\beta = 0°$, shown at (a,e) $x/D = 4$, (b,f) $x/D = 6$, (c,g) $x/D = 8$, and (d,h) $x/D = 10$. The blue triangle inverted triangles (∇) and the black solid line ($-$) show the contour line at $\Delta U/U_{\infty,h} = 0.1$ from the LES data and analytical model (with $\alpha_k = 0.4$), respectively.

wake extents identified by the $\Delta U/U_{\infty,h} = 0.1$ contour line are severely under-predicted by the analytical model as compared to the LES.

Analogous and complementary results are seen in Figure 5 for $\beta = -41.3°$. Specifically, reflecting the contours obtained for the $(\beta,\gamma) = (41.3°,30°)$ case along the vertical axis would yield results very similar to those seen for the $(-41.3°,-30°)$ case. Similarly, complementary results are seen between the $(\beta,\gamma) = (41.3°,-30°)$ and $(-41.3°,30°)$ cases as well.

Centerline Velocity Deficit and Power

Figure 6 shows the evolution of the streamwise velocity deficit along the wake centerline for all nine cases simulated here. While the wake shapes and deflections are very different across the nine cases as described above, the velocity deficit along the centerline is largely the same across all values of latitude β for a fixed yaw misalignment γ. Furthermore, comparing Figures 6b and 6c, it is clear that the centerline velocity deficit evolution is the same for positively- and negatively-yawed turbines for $\beta = 0°$ and $-41.3°$. Differences are seen only for the $(\beta,\gamma) = (41.3°,30°)$ case and the other cases. Predictions of the analytical model are independent of the latitude and are in close agreement with the LES data in most of the cases with small discrepancies seen only beyond $x/D = 10$ where the wake deficit magnitude is quite small, around $\Delta U_c/U_{\infty,h} = 0.1 - 0.15$. We note that this good agreement is partly due to parameter tuning. The wake expansion coefficient, k is selected by choosing a value for α_k such that good agreement with the LES results is obtained for the centerline velocity deficit evolution.

Figure 7 shows the streamwise evolution of the normalized power that a hypothetical turbine located behind the turbine would generate. The normalized power is given by

$$\frac{P}{P_0} = \left(\frac{U_{d,avg}}{U_{\infty,m}}\right)^3 \qquad (2)$$

where P is the available power of the hypothetical turbine, P_0 is the power available for a non-yawed turbine exposed to the fresh wind $U_\infty(z)$. $U_{d,avg}$ and $U_{\infty,m}$ are the streamwise wind speed averaged over the rotor-disk area of the hypothetical turbine, and at the upstream of the non-yawed turbine, respectively. For $\gamma = 0°$ (Figure 7a), the LES data show only a weak dependence on the latitude. The slight distortion caused by wind veer leads to marginally larger power for the $\beta = \pm 41.3°$ cases over the $\beta = 0°$ case. Furthermore, the model predictions agree reasonably well with the LES data for these cases. For $\gamma = -30°$ (Figure 7b), the power profiles differ considerably with changing latitude. The differences arise because of the interaction between yaw-induced counter-rotating vortex pairs and Coriolis force-induced wind veer, that lead to either an almost-Gaussian or a curled wake shape as discussed above. When averaged over the turbine rotor, the available power values are larger for the almost Gaussian-like shape of $\gamma = -41.3°$ than for the curled wake shape of $\gamma = 41.3°$. Similarly, for $\gamma = 30°$ (Figure 7c) cases, the power is largest for the near-Gaussian shape observed for $\beta = 41.3°$ and smallest for the curled wake of $\beta = -41.3°$. The analytical model results are mostly insensitive to β and agree with the available power values obtained from the LES of the $(\beta,\gamma) = (-41.3°,-30°)$ and $(41.3°,30°)$ cases, respectively.

SUMMARY AND CONCLUSIONS

The effect of latitude on yawed and non-yawed isolated turbines is investigated using large eddy simulations. The wake shape is seen to be affected by the latitude as well as the yaw misalignment direction. The wake of a non-yawed turbine is a symmetric Gaussian in the absence of Coriolis-induced wind veer (for a turbine located on the equator) and is an asymmetric skewed Gaussian for non-zero latitudes. When the latitude as well as the yaw misalignment angle are both positive or both negative, the wake shape remains similar to, but is not exactly, a skewed Gaussian. When the latitude is positive (negative) and the yaw misalignment is negative (positive), a distinct curled wake shape is observed as seen in previous studies.

An analytical modeling framework reported in previous studies (Bastankhah *et al.* (2022) and Mohammadi *et al.* (2022)) predicts wake shapes that are broadly reasonable, but the precise extents of the wake edge are not predicted correctly. The centerline velocity deficit is not sensitive to the latitude in the LES as well as model predictions. The LES results further show that the power available for a hypothetical wind turbine placed in the wake of an upstream turbine is, however, signif-

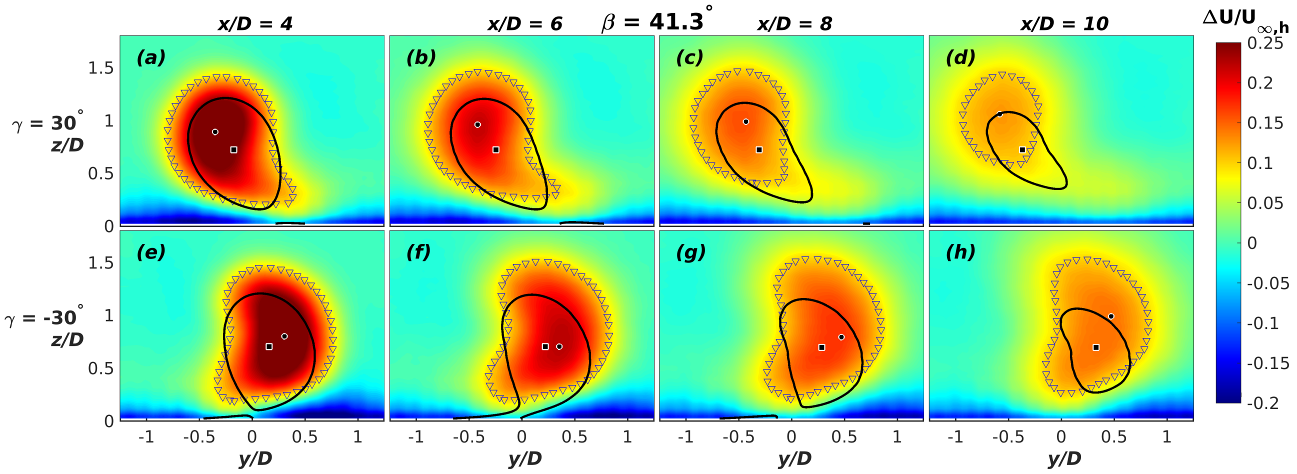

Figure 4. Spatial variation of contours downstream of a turbine yawed at, (a-d) $\gamma = 30°$ and (e-h) $\gamma = -30°$ located at latitude $\beta = 41.3°$, shown at (a,e) $x/D = 4$, (b,f) $x/D = 6$, (c,g) $x/D = 8$, and (d,h) $x/D = 10$. The blue triangle inverted triangles (∇) and the black solid line ($-$) show the contour line at $\Delta U/U_{\infty,h} = 0.1$ from the LES data and analytical model (with $\alpha_k = 0.4$), respectively.

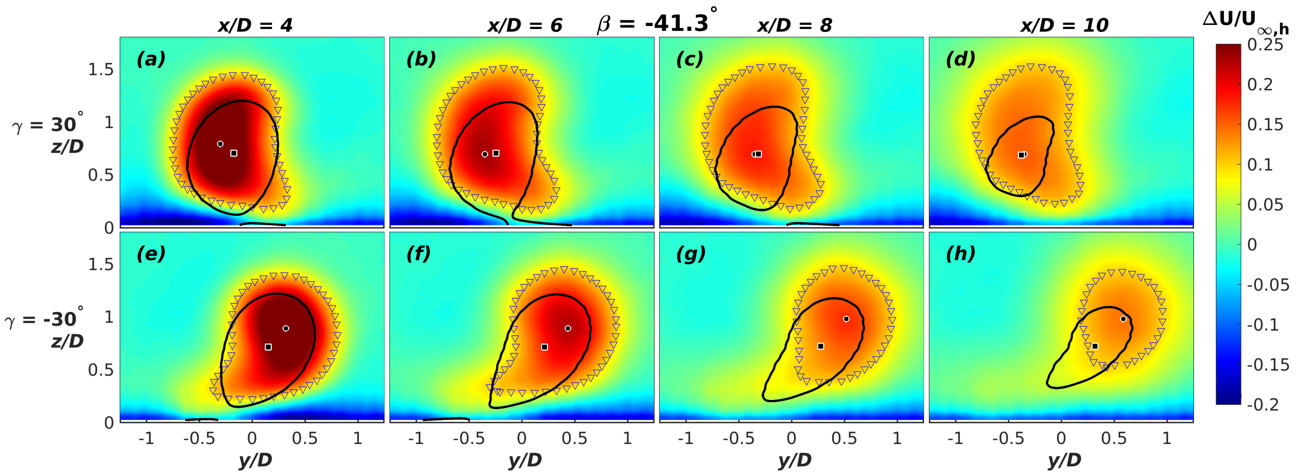

Figure 5. Spatial variation of contours downstream of a turbine yawed at, (a-d) $\gamma = 30°$ and (e-h) $\gamma = -30°$ located at latitude $\beta = -41.3°$, shown at (a,e) $x/D = 4$, (b,f) $x/D = 6$, (c,g) $x/D = 8$, and (d,h) $x/D = 10$. The blue triangle inverted triangles (∇) and the black solid line ($-$) show the contour line at $\Delta U/U_{\infty,h} = 0.1$ from the LES data and analytical model (with $\alpha_k = 0.4$), respectively.

icantly affected by the latitude as well as the yaw angle of the upstream turbine. The analytical model predictions, however, agree with the LES results only when the latitude and yaw misalignment are either both positive of both negative.

Future work will focus on improvements to the analytical model for obtaining correct wake extents and obtaining good quantitative predictions of the power for positive and negative latitudes and yaw misalignment angles.

ACKNOWLEDGEMENTS

UDT kindly acknowledges the support provided by the Prime Minister's Research Fellowship, Ministry of Education, Government of India. NSG thanks the SERB Core Research Grant (CRG/2022/006735). KM would like to thank the Department of Science and Technology (DST), Government of India, for the support provided by the project (DST/NSM/R&D_HPC_Applications/2021/23) under the National Supercomputing Mission (NSM). The authors thank the computational resources on ParamSeva at IIT Hyderabad.

REFERENCES

Abkar, M. & Porté-Agel, F. 2016 Influence of the coriolis force on the structure and evolution of wind turbine wakes. *Physical Review Fluids* **1**.

Bastankhah, M., Shapiro, C. R., Shamsoddin, S., Gayme, D. F. & Meneveau, C. 2022 A vortex sheet based analytical model of the curled wake behind yawed wind turbines. *Journal of Fluid Mechanics* **933**, A2.

Churchfield, M. J., Lee, S., Michalakes, J. & Moriarty, P. J. 2012 A numerical study of the effects of atmospheric and wake turbulence on wind turbine dynamics. *Journal of Turbulence* **13**, N14.

Fleming, P. A., Gebraad, P. M. O., Lee, S., van Wingerden, J.-W., Johnson, K., Churchfield, M., Michalakes, J., Spalart, P. & Moriarty, P. 2014 Evaluating techniques for redirecting turbine wakes using sowfa. *Renewable Energy* **70**, 211–218.

Heck, K. S. & Howland, M. F. 2025 Coriolis effects on wind turbine wakes across neutral atmospheric boundary layer regimes. *Journal of Fluid Mechanics* **1008**.

Howland, M. F., Bossuyt, J., Martínez-Tossas, L. A., Meyers, J. & Meneveau, C. 2016 Wake structure in actuator disk models of wind turbines in yaw under uniform inflow con-

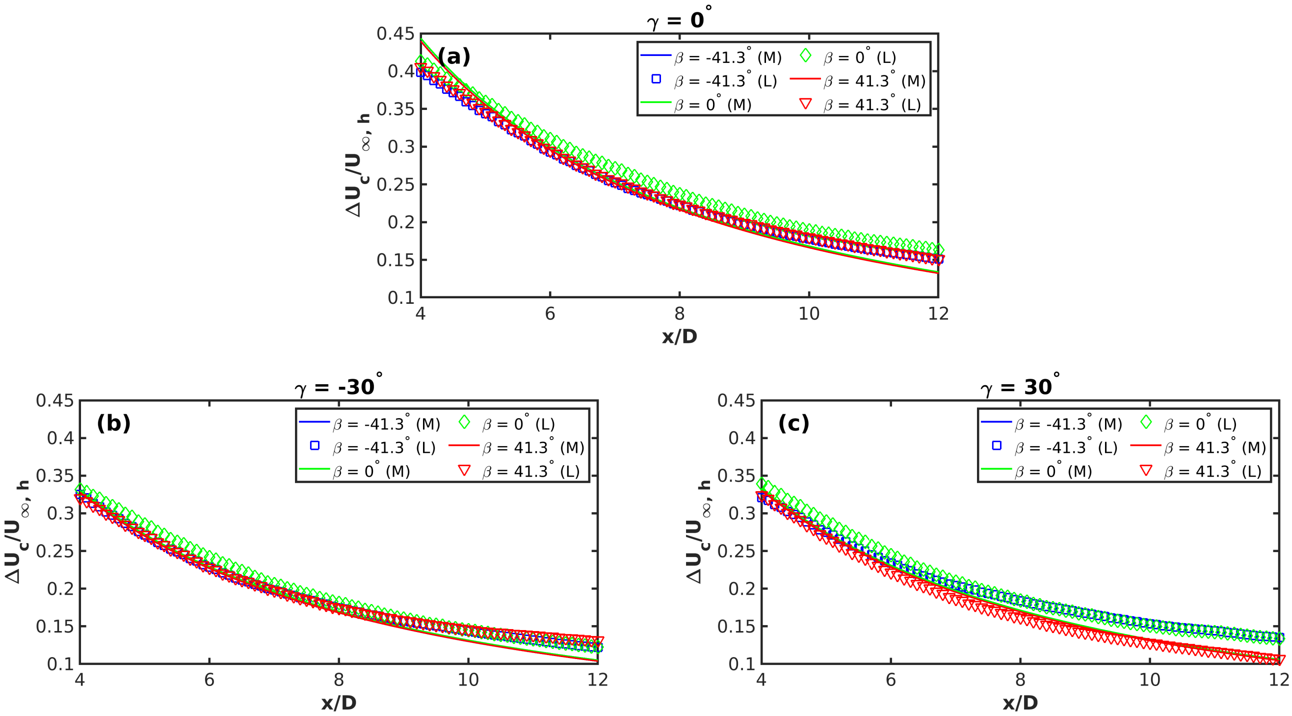

Figure 6. Variation of normalized wake centerline velocity deficit along the downstream direction for turbines yawed at (a) $\gamma = 0°$, (b) $\gamma = -30°$, and (c) $\gamma = 30°$ at different latitudes, β. The tunable parameter α_k is (a) 0.5 and (b, c) 0.4.

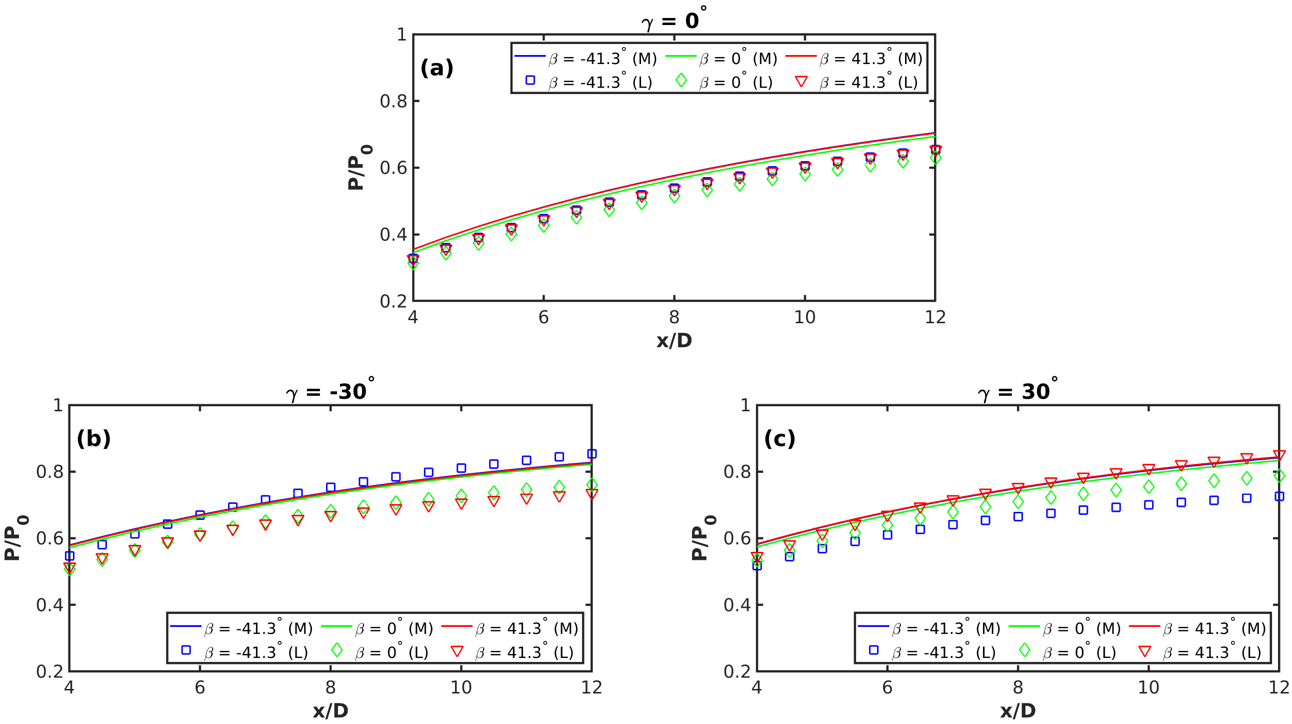

Figure 7. Normalized power output of an imaginary turbine located downstream of a turbine yawed at (a) $\gamma = 0°$, (b) $\gamma = -30°$, (c) $\gamma = 30°$ at different latitudes. The tunable parameter α_k is (a) 0.5 and (b, c) 0.4.

ditions. *Journal of Renewable and Sustainable Energy* **8**, 043301.

Mohammadi, M., Bastankhah, M., Fleming, P., Churchfield, M., Bossanyi, E., Landberg, L. & Ruisi, R. 2022 Curled-skewed wakes behind yawed wind turbines subject to veered inflow. *Energies* **15**.

Tiwari, U. D., Ghaisas, N. S. & Mitra, K. 2025 Evaluating the combined effect of yaw misalignment and wind farm column misalignment on wake losses in finite wind farm arrays using large eddy simulation. *Physics of Fluids* **37**, 105135.